Electric Power Systems Research 129 (2015) 114–125

Contents lists available at ScienceDirect

Electric Power Systems Research

journal homepage: www.elsevier.com/locate/epsr

Review

Applying conservative power theory for analyzing three-phase X-ray machine impact on distribution systems

Alexandre C. Moreira [a,*], Helmo K.M. Paredes [b], Luiz C.P. da Silva [a]

[a] University of Campinas (UNICAMP), School of Electrical and Computer Engineering (FEEC), Department of Systems and Energy (DSE), Av. Albert Einstein, 400, 13083-852 Campinas, SP, Brazil
[b] Univ Estadual Paulista (UNESP), Campus of Sorocaba, Group of Automation and Integrated Systems (GASI), Av. Três de Março, 511, 18087-180 Sorocaba, SP, Brazil

ARTICLE INFO

Article history:
Received 3 March 2015
Received in revised form 20 July 2015
Accepted 27 July 2015
Available online 27 August 2015

Keywords:
Conservative power theory
Non-linear loads
Power quality
X-ray

ABSTRACT

This article proposes the use of the conservative power theory as an alternative tool to analyze and determine the possible impacts of noisy loads on electrical distribution systems. The orthogonal decomposition of current (or power) of the conservative power theory allows the definition of different performance factors, each factor represents a specific feature of the load (current lag behind the voltage, unbalance and harmonic distortion). Each factor is used to identify potential effects of the X-ray machine on the system. Furthermore, a computational model developed in PSCAD/EMTDC of the three-phase X-ray machine is presented. The analysis and discussions are based on simulations and actual measurements obtained on the terminals of an X-ray machine. The presented results helps to demonstrate the main advantage of the CPT compared to conventional approaches, which is related to its general application for single phase and poly-phase circuits, for asymmetrical and distorted supply voltages, for nonlinear and unbalanced loads and, for variable line frequency.

Contents

* Corresponding author. Tel.: +55 15 98126 4356.
E-mail addresses: alexandre.candido.moreira@gmail.com (A.C. Moreira), hmorales@sorocaba.unesp.br (H.K.M. Paredes), lui@dsee.fee.unicamp.br (L.C.P. da Silva).

http://dx.doi.org/10.1016/j.epsr.2015.07.019
0378-7796/

1. Introduction

Power Electronic (PE) is entering in a consolidated age, not only in the industrial sector but also in many other areas, bringing advantages in the processing of energy (more effective). On the other hand, due to this wide spread of PE, the level of harmonics and voltage and/or current asymmetries is increasing drastically, not only in industrial and commercial activities, but also for domestic use, causing disturbances in the distribution and consumption of electrical energy [1,2]. Thus, this subject has become extremely important especially regarding measurement issues, revenue metering and power quality (PQ) [3–6].

In this scenery, in recent decades, the use of X-ray machine has grown, mainly due to the development of portable appliances with lower cost and easy handling. Usually, no information is given to the power utility about their existence or utilization regime. Given their (nonlinear) constructive features, this type of device is considered as a potentially disturbing load [7,8]. It can bring many problems to the distribution system and PQ degradation.

This aspect has been reason of studies and discussions by the utilities and standards [3,6,9,10] that include, among other power quality indicators, the topic of harmonics distortions, load unbalance and power factor. In accordance to these orientations, and recognizing that the solutions to the adequacy of the performance indicators involve financial costs, appears the question of finding ways to determine the responsibilities for eventual violations of the pre-established limits for harmonic distortions, load unbalance and power factor. So, many researchers have been directing their efforts to propose new definitions and theories, able to be applied to non-sinusoidal and/or asymmetric conditions [3,5,11–16]. In practice, such a reassessment would produce impact on various applications such as compensation techniques, revenue metering, instrumentation, etc.

In this sense, the conservative power theory (CPT), presented in [5,11] is used to assess potential impacts caused by the X-ray machine on power systems, with focus on the PQ evaluation. The CPT proposes the orthogonal current/power decomposition in time domain, where each current/power component can be related to a specific load performance factors (PQ index), which allows to identify and to quantify the amount of resistive, reactive, unbalance and nonlinear characteristics of a particular load under different supply voltages condition [19]. In fact, as it will be discussed, this is quite different from using traditional PQ indexes, such as: displacement factor, negative and zero sequence factors or total harmonic distortion (THD). The load performance factors follow the same idea to traditional PQ indexes, however focusing on the identification and quantification of the load phenomena at the point of common coupling (PCC). Therefore, the CPT factors (load performance factors) represent the information of how the generic load circuits affect the current and power terms at the PCC. Besides, their information is related to the entire three-phase circuit, not to single phase variables. Furthermore, the developed model and its implementation in PSCAD™/EMTDC™ software can be employed on power quality studies for exploring the load characteristic. The X-ray is modeled based on field measurement data obtained from a Brazilian university hospital [17,18]. Thus, this model and CPT PQ indices are used to discuss and analyze the possible impacts of the X-ray machine on distribution systems.

2. Description of X-ray current waveforms

The X-ray machine has two operation modes: continuous and momentary. During the operation in momentary mode at the time of radiography, the electrical power required is high and it can produce voltage sags or even damage the operation of other sensitive equipment connected to the circuit. Fig. 1a shows the load terminals instantaneous currents measured in an X-ray GE Yokogawa Medical System (Model 2137298) equipment during the execution of radiographies.

From Fig. 1b it is observed that the instantaneous current presents four different areas of operation:

- *Area A:* in this time zone the amplitudes of the instantaneous currents are minimal, showing that the device is energized, but there is no voltage being applied to the filament of X-ray tube;
- *Area B:* it is observed that the amplitude of the current increases, the equipment operator sends a command to perform an X-ray radiograph;
- *Area C:* in this time zone the execution of the radiography occurs, which causes a considerable increase in the amplitude of the instantaneous current (reaching maximum values), and thus originate a voltage sag;
- *Area D:* after execution of the radiography the device returns to its initial state, being just energized and waiting for the next execution command. The machine returns to the initial state (Area A) as an execution of one cycle.

For a better understanding of each operation area, in the following sections it will be presented all the circuits that compose the model of the X-ray machine.

3. Computational modeling of X-ray machine

As described in [7,18], the model of X-ray device (GE Yokogawa Medical System – Model 2137298) was implemented in PSCAD™/EMTDC™ software and can be divided into three basic circuits:

- Filament supply circuit;
- Electronic control supply circuit;
- High-voltage supply circuit.

This configuration was adopted to enable the complete representation of the X-ray machine and shows in Fig. 2. Fig. 2a shows the supply circuit of the filament of the X-ray tube. This is the simplest circuit of the machine, consists of only an electrical resistance which is the filament of the X-ray tube.

The electronic control systems (Fig. 2b) generally require a low voltage DC (direct current) supply between 5 and 12 V [18]. Therefore the supply circuit was modeled by a three-phase 6-pulse rectifier followed by a LC filter (used to remove the voltage ripple) and a resistance representing the element which consumes electrical power.

Finally, Fig. 2c shows the circuit responsible for generating the necessary voltage to create the electric arc inside the tube. It is composed by a three-phase voltage transformer, 220 V to 100 kV and a 6-pulse bridge rectifier, used for rectifying the voltage. The parallel branch to the device's tube is responsible for loading the capacitor which will maintain a stable level of voltage in the tube during the electrical discharge. The consideration of this branch is essential for the correct representation of the device. It is worth highlighting that the electric model of GE Yokogawa Medical System (Model 2137298) is not available in the literature.

4. Impact evaluation of X-ray on electric power distribution systems

A typical configuration of the electrical network for a Brazilian university hospital was considered to analyze and quantify the impacts caused by X-ray machine. Fig. 3 shows the topology and its

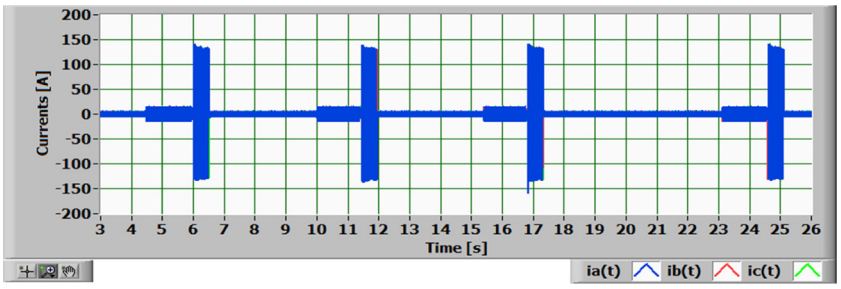

a) Four X-ray radiographs performed.

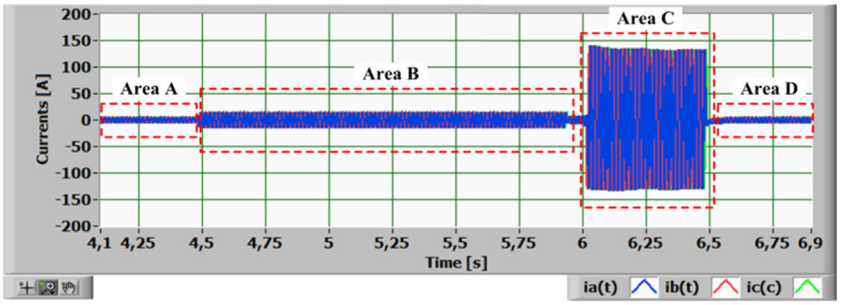

b) One X-ray radiograph (zoom-in).

Fig. 1. Field measurement X-ray instantaneous currents.

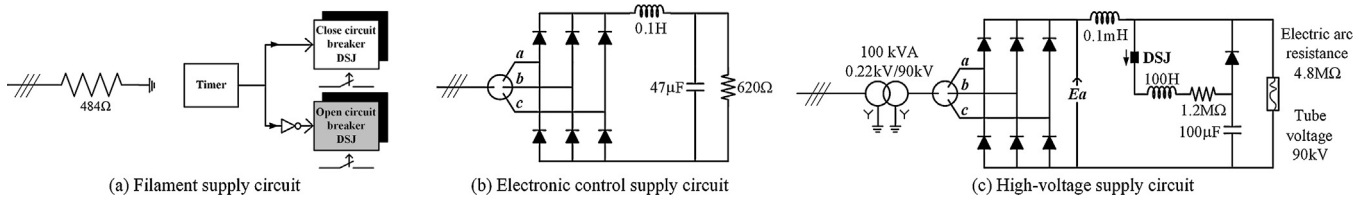

(a) Filament supply circuit (b) Electronic control supply circuit (c) High-voltage supply circuit

Fig. 2. Basic electrical circuits to modeling X-ray machine.

components. This is composed by a three-phase supply, a series RL circuit representing the impedance of the line, a step-down star-delta transformer responsible for feeding of the device. The short-circuit capacity ($S_{CC} = 100$ MVA) was provided by the utility, as well as the ratio $\left(\frac{X}{R} = 4\right)$. In this way is possible to represent the utility by means the source and the equivalent series impedance. All parameters of the topology are specified on Table I.

Fig. 4 shows the waveforms at the point of common coupling (PCC) and on the apparatus terminals, secondary of the transformer (load), for each operation area. This analysis gives an overview of the possible impacts of the X-ray machine in the electrical system, into two different scenarios, for example in a hospital (PCC) and an office (load).

For analytical purposes will be considered the following time intervals:

- Between $t = 0.00$ s to $t = 1.00$ s – Area A;
- Between $t = 1.00$ s to $t = 2.03$ s – Area B;
- Between $t = 2.03$ s to $t = 2.55$ s – Area C;
- And $t = 2.55$ s and forward – Area D.

4.1. Analysis of Area A

It is observed in Fig. 4a that, as expected, the current is minimum, representing the situation in which the device is only energized, waiting for the operator command to execute a radiography. But it is observed that, there is a difference in the current distortion between the PCC (low harmonic content) and the load terminals (high harmonic content).

The rms values of the phase currents are shown in Table II. It is noticed that, depending on the point of measurement, the current distortions are quite different. For example, if the device is used in the hospital (PCC), the current distortion gets around 4%. However

Table I
Voltages and impedances.

Source (kV)	Line	Transformer
$V_{an} = 7.97 \angle 0°$	$R_a = R_b = R_c = R$	150 kVA
$V_{bn} = 7.97 \angle -120°$	$L_a = L_b = L_c = L = 4.9$ mH	13.8 kV/220 V
$V_{cn} = 7.97 \angle +120°$	$R = 0.462\ \Omega$; $X = j1.847\ \Omega$	Δ/Y

Table II
Simulation results (Area A).

Phase	Currents rms value (A)		THD (%)	
	PCC	Load	PCC	Load
a	0.074	0.674	3.96	18.69
b	0.070	0.735	3.98	18.69
c	0.079	0.771	3.94	18.70

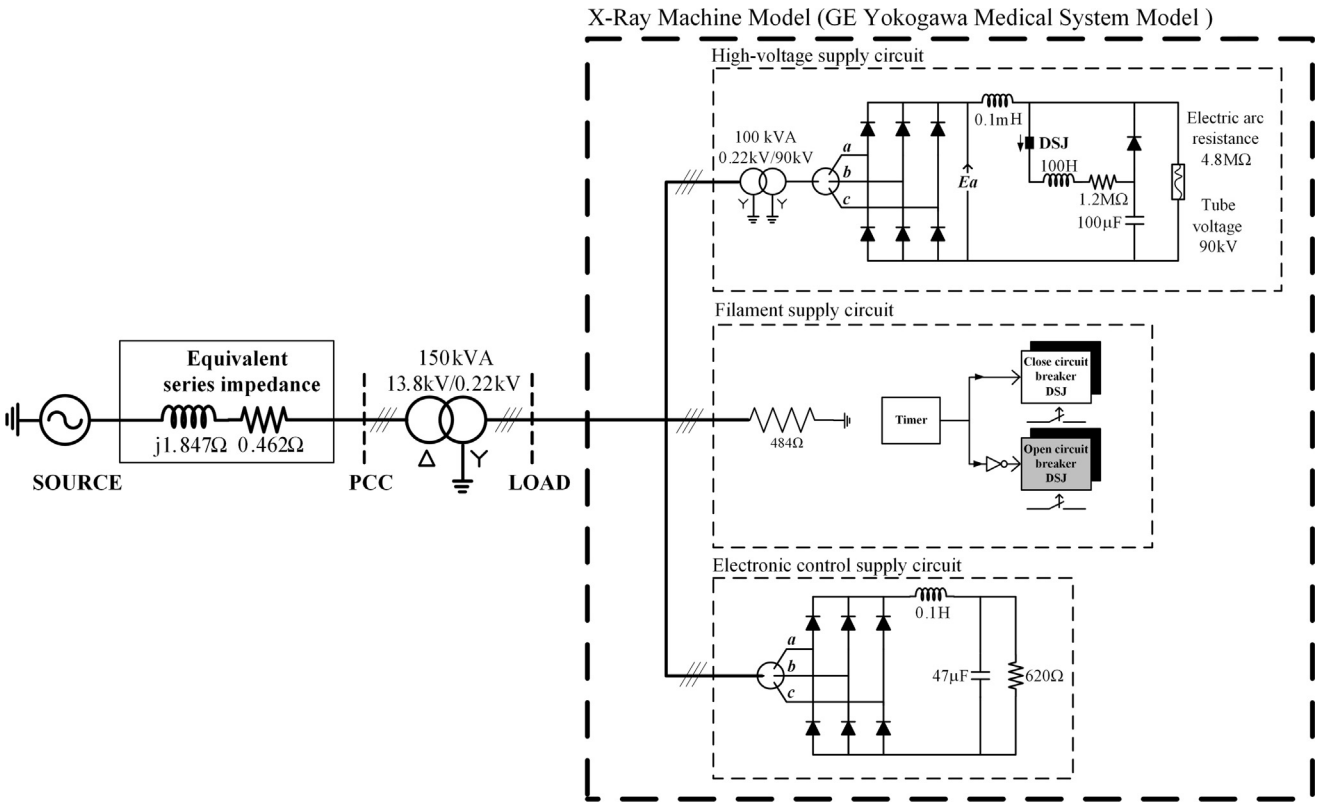

Fig. 3. Scheme of electrical network.

if the same device is used in a private office (load), the distortion reaches to approximately 19%.

Fig. 5a shows the harmonic spectrum into the terminal of the device (load). It can be observed that the harmonics characteristics are in the 5th, 7th, 11th and 13th order.

4.2. Analysis of Area B

From Fig. 4b, it is noticeable that, in this time zone of operation, differently than on Area A, the amplitudes of the currents in both measurement points (PCC and in the load terminals) increased. It is more distorted especially in the PCC, compared to Area A. The difference in the waveforms in the measurement points is due to the Δ/Y transformer, which causes phase shift in the phases of harmonic currents.

Table III shows the rms values of the phase currents and THDs.

Table III
Simulation results (Area B).

Phase	Currents rms value (A)		THD (%)	
	PCC	Load	PCC	Load
a	0.251	11.11	19.86	26.23
b	0.235	11.94	19.84	26.23
c	0.267	12.66	19.94	26.23

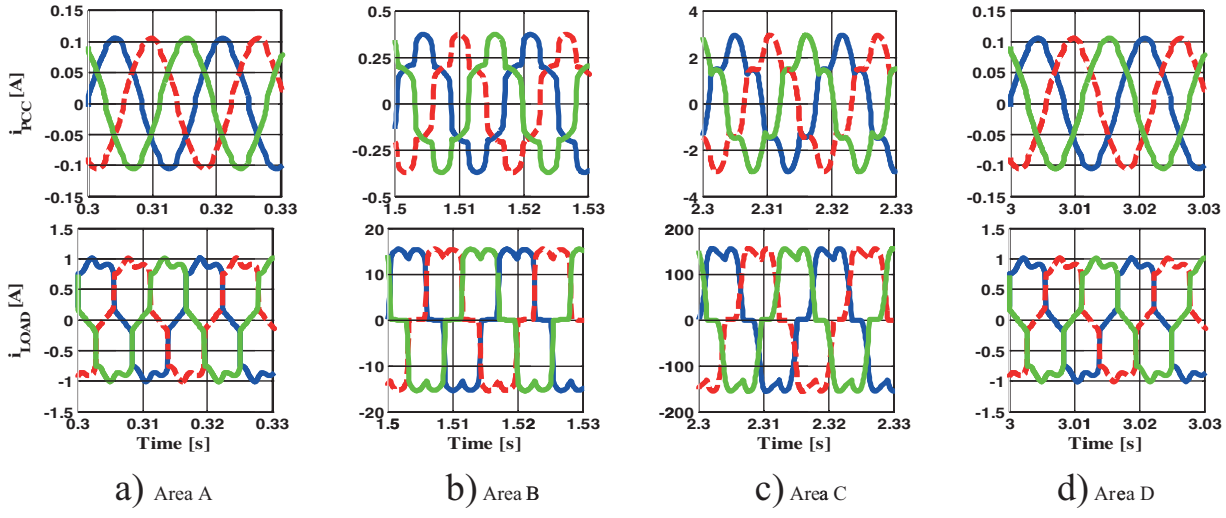

Fig. 4. Line currents waveform at PCC and Load currents waveform for each X-ray operation area.

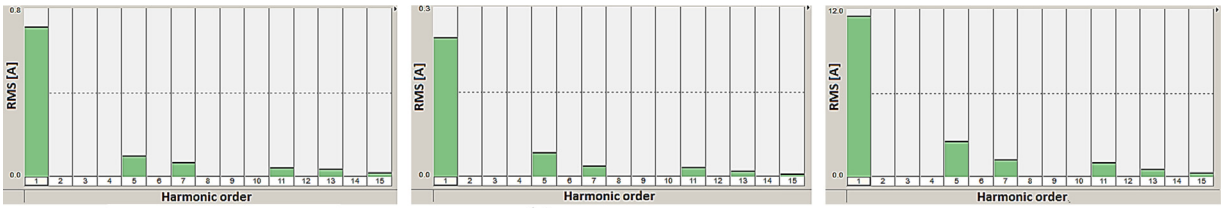

Fig. 5. FFT of current waveform (phase *a*).

Table IV
Simulation results (Area C).

Phase	Currents rms value (A)		THD (%)	
	PCC	Load	PCC	Load
a	1.898	111.605	20.27	20.96
b	1.795	113.578	20.28	20.95
c	1.975	122.258	20.27	20.95

Table V
Simulation results (Area D).

Phase	Currents rms value (A)		THD (%)	
	PCC	Load	PCC	Load
a	0.011	0.669	3.96	18.70
b	0.011	0.732	3.98	18.61
c	0.012	0.767	3.94	18.51

This area represents the region where the operator of the machine will send the command for the execution of radiography, where the effective current in the PCC increased from 0.074 A (Table II) to approximately 0.251 A (Table III) and at the load terminals the current increased from approximately 0.73 A to 11 A. Fig. 5b and c shows the harmonic spectrum into the PCC and terminal of the device (load) for Area B. It can be observed that the harmonics characteristics are in the 5th, 7th, 11th and 13th order.

4.3. Analysis of Area C

We must remember that this area represents the moment of execution of the radiography. Therefore, in this time zone we have a high level of voltage inside the X-ray tube which causes the creation of the electric arc, increasing the amplitude of the currents. Fig. 4c shows the waveform of the current at the PCC and at load terminals. It is observed that in fact the amplitude of currents in the PCC and at load terminals increases 10 times higher than in region B, which is reaching 3 A at PCC and 150 A at load terminals.

Fig. 6 shows the harmonic spectrum of the phase current. We notice that the harmonics characteristics are the same (on 5th, 7th, 11th and 13th) of the preceding areas (A and B), which means that the harmonics remain during the operation of the equipment, but the amplitudes vary by area on which such apparatus operates.

In Table IV the rms values of the phase currents and the total harmonic distortion are represented for each phase. It is verified that, in this time zone the THDs are roughly equivalent at the measuring points (PCC and load), representing a total harmonic content of approximately 21%. Furthermore, it is observed that the rms value of the current comes to be approximately 112 A at the load terminals and 1.8 A in the PCC.

4.4. Analysis of Area D

From Fig. 4d, it is noted that in this area the X-ray machine returns to its initial state representing the same waveforms and amplitudes as in Area A. On the other hand, from Table V, we observe that the rms values of current and THDs are practically the same as in Area A, indicating that the device returns to the initial operating condition and is ready to execute the next operator command for another X-ray radiograph.

From the foregoing analysis, it is evident that the impact of X-ray machine depends on the connection point. For example, if it is used in a private office (analysis at the load terminals) the machine shows levels of harmonic distortion that can oscillate between 19% and 27% over the four areas of operation. In the case of the PCC analysis (e.g., equipment used in a hospital) the levels of harmonic distortion is significant just for Areas B and C with distortion levels of approximately 20%. Therefore, this difference in the operating characteristic of the X-ray machine can influence in the calculation of the power factor and on the power quality analysis of the installation. In the following section, it will be presented the orthogonal current/power decomposition of the CPT, in order to calculate the effects of the X-ray machine in the involved quantities, for later discussion and examinations.

5. CPT power and currents decompositions

The conservative power theory (CPT) developed in the time domain in [5,11] is based on the orthogonal decomposition of the current. The CPT provides a physical interpretation of the power phenomena in single phase and poly-phase (with and without return conductor) systems under non-ideal conditions, i.e., with asymmetrical and distorted supply voltages, nonlinear and unbalanced loads and, possibly, variable line frequency. Let us assume

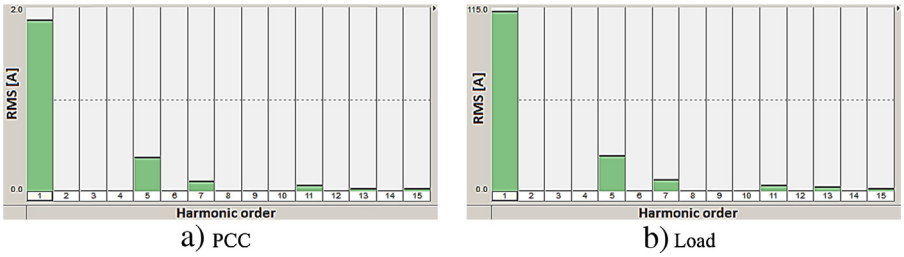

Fig. 6. FFT of current waveform (phase *a*) (Area C).

a multiphase circuit where each phase voltage and current are denoted by the subscript "m" and the variables in bold indicate the representation of a multidimensional vector (three-dimensional in the three-phase case).

The *instantaneous power* was defined by the scalar product:

$$p = \boldsymbol{v} \circ \boldsymbol{i} = \begin{bmatrix} v_a & v_b & v_c \end{bmatrix} \circ \begin{bmatrix} i_a \\ i_b \\ i_c \end{bmatrix}, \tag{1}$$

while the instantaneous reactive energy was defined as:

$$w = \hat{v} \circ \boldsymbol{i} = \begin{bmatrix} \hat{v}_a & \hat{v}_b & \hat{v}_c \end{bmatrix} \circ \begin{bmatrix} i_a \\ i_b \\ i_c \end{bmatrix}, \tag{2}$$

where $\hat{\boldsymbol{v}}$ is defined as the vector containing the unbiased integrals of the phase voltages. In other words, this quantity $\hat{\boldsymbol{v}}$ is calculated by the difference between the time integral and its average value, as shown below:

$$\begin{aligned} &\hat{v}_m(t) = v_{\text{int\_}m} - \bar{v}_{\text{int\_}m} \quad m \in \{a, b, c\} \\ &v_{\text{int\_}m} = \int_t v_m(t)dt \\ &\bar{v}_{\text{int\_}m} = \frac{1}{T}\int_0 v_{\text{int\_}m}(t)dt \end{aligned} \tag{3}$$

where $v_{\text{int\_}m}$ is the integral of the voltage and $\bar{v}_{\text{int\_}m}$ is the mean value of $v_{\text{int\_}m}$.

Considering the mean values of (1) and (2) following quantities were defined:

- Active power:

$$P = \bar{p}(t) = \frac{1}{T}\int_0^T \left(\begin{bmatrix} v_a & v_b & v_c \end{bmatrix} . \begin{bmatrix} i_a \\ i_b \\ i_c \end{bmatrix} \right) dt \tag{4}$$

  This definition is identical to the one of the conventional active power [3,12,13,15,16] and represents the average power consumption. Note that, in sinusoidal conditions, the term P coincides, at any moment, with classical active power $P = VI\cos\emptyset$.
- Reactive energy:

$$W_r = \bar{w}_r(t) = \frac{1}{T}\int_0^T \left(\begin{bmatrix} \hat{v}_a & \hat{v}_b & \hat{v}_c \end{bmatrix} . \begin{bmatrix} i_a \\ i_b \\ i_c \end{bmatrix} \right) dt \tag{5}$$

The reactive energy, in turn, is a new quantity, which relates the average energy stored in the multiphase circuit in generic conditions, and only sinusoidal with constant frequency condition can be associated with the conventional reactive power ($W_r = W_r = \frac{Q}{\omega} = \frac{1}{\omega}VI\sin\emptyset$), where $\emptyset$ is the angle difference between voltage and current, and ω the grid frequency. Thus, conventional reactive power is associated with the frequency of the electrical grid, whereas the reactive energy proposed by the CPT is independent of frequency, making it interesting for systems with possible frequency variations, such as microgrids. From a practical perspective, it suffices for the average value of Eqs. (2) and (3) to be calculated by means of frequency adaptive algorithms or simply low-pass filters, so that both the active power and the reactive energy are immune to variations in mains frequency. In addition, the variables (voltages and currents, as well as their integrals and derivatives) defined by the authors of the CPT satisfy Kirchhoff's Voltage and Current Laws. Thus, according to Tellegen's Theorem, it can be stated that each dot product of these variables is a conservative quantity, which allows for the introduction of the concept of active power and reactive energy conservation in any grid regardless of voltages and current waveforms (unbalance and/or harmonic distortion) [5,11].

Based on the definitions of active power and reactive energy, the instantaneous current at PCC can be decomposed into the following orthogonal components:

Active phase currents is defined as the minimum current (i.e., with minimum rms value) needed to convey active power P_m measured at PCC. It given by:

$$i_{am} = \frac{P_m}{V_m^2}v_m = G_m v_m \quad m \in \{a, b, c\} \tag{6}$$

where $G_m = P_m/V_m^2$ is the *equivalent phase conductance* and V_m is the rms voltage value per phase respectively.

Reactive phase currents is defined as the minimum current (i.e., with minimum rms value) needed to convey reactive energy W_m measured at PCC. It given by:

$$i_{rm} = \frac{W_{rm}}{\hat{V}_m^2}\hat{v}_m = B_m \hat{v}_m \quad m \in \{a, b, c\} \tag{7}$$

where $B_m = W_{rm}/\hat{V}_m^2$ is the *equivalent phase reactivity* and $\hat{V}_m$ is the rms value of the unbiased integral of the voltage per phase.

Void phase currents are the terms of remaining currents:

$$i_{vm} = i_m - i_{am} - i_{rm} \quad m \in \{a, b, c\} \tag{8}$$

where i_m is the phase total current at PCC. The meaning of void currents was explained in [21]. These current terms do not transmit active power neither reactive energy and represent harmonic currents generated by the load (harmonic terms that only exist in current spectrum) and the scattered harmonic currents (caused by voltage harmonics), that are due to different values of conductance and reactivity in different harmonics.

In general, the active and reactive currents can be still decomposed into balanced and unbalanced terms. The balanced terms refer to a balanced equivalent circuit that transmits all active power and all reactive energy and are expressed by:

Balanced active currents are the minimum currents (with minimal collective rms value), necessary to transfer total active power (P) to the load, and are defined:

$$i_{am}^b = \frac{P}{\boldsymbol{V}^2}v_m = \left(\frac{P}{V_a^2 + V_b^2 + V_c^2}\right)v_m = G^b v_m \tag{9}$$

where $\boldsymbol{V} = \sqrt{V_a^2 + V_b^2 + V_c^2}$ is the collective rms value of the voltage and parameter G^b is the *equivalent balanced conductance*. Note that the balanced active currents (i_{am}^b) are proportional to v_m, this means that the balanced active currents have the same waveform and always will be in phase with the voltages.

Balanced reactive currents are the minimum currents (with minimal collective rms value) necessary transfer total reactive energy, and are given by:

$$i_{rm}^b = \frac{W_r}{\hat{\boldsymbol{V}}^2}\hat{v}_m = \left(\frac{W_r}{\hat{V}_a^2 + \hat{V}_b^2 + \hat{V}_c^2}\right)\hat{v}_m = B^b \hat{v}_m \tag{10}$$

where $\hat{\boldsymbol{V}} = \sqrt{\hat{V}_a^2 + \hat{V}_b^2 + \hat{V}_c^2}$ is the collective rms value of unbiased integral of the voltage and parameter B^b is the *equivalent balanced reactivity*. In this case, the balanced reactive currents are proportional to the integrals without mean value of voltage. Thus, i_{rm}^b contain all the information about the phase shift between the voltages and currents, not only caused by storage elements (inductors and capacitors), but also caused by nonlinear loads.

Unbalanced currents: are composed by active and reactive terms that represent the different values of load conductance and reactivity by phase and it is given by:

$$i_m^u = i_{am}^u + i_{rm}^u = (G_m - G^b)v_m + (B_m - B^b)\hat{v}_m \tag{11}$$

it is observed that those currents only exist if the equivalent conductances and reactivities of phases differ from each other, in other words when the load is unbalanced.

So, as all the current components are orthogonal [5,11], the instantaneous current and the collective rms value of current, can be decomposed as:

$$i_m = i_{am} + i_{rm} + i_{vm} = i_{am}^b + i_{rm}^b + i_m^u + i_{vm} \tag{12}$$

$$\boldsymbol{I}^2 = \boldsymbol{I}_a^2 + \boldsymbol{I}_r^2 + \boldsymbol{I}_v^2 = \boldsymbol{I}_a^{b\,2} + \boldsymbol{I}_r^{b\,2} + \boldsymbol{I}^{u\,2} + \boldsymbol{I}_v^2 \tag{13}$$

Multiplying (13) by the square of the collective rms value of the voltage, the apparent power can be decomposed into:

$$A^2 = \boldsymbol{V}^2\boldsymbol{I}^2 = \boldsymbol{V}^2\boldsymbol{I}_a^{b\,2} + \boldsymbol{V}^2\boldsymbol{I}_r^{b\,2} + \boldsymbol{V}^2\boldsymbol{I}^{u\,2} + \boldsymbol{V}^2\boldsymbol{I}_v^2 \tag{14}$$

$$A^2 = P^2 + Q^2 + N^2 + D^2 \tag{15}$$

where:

$$P = \boldsymbol{V}\boldsymbol{I}_a^b = \sqrt{\left(V_a^b + V_b{}^2 + V_c{}^2\right)\left(I_{aa}^{b\,2} + I_{ab}^{b\,2} + I_{ac}^{b\,2}\right)} \tag{16}$$

is the ***active power***. This power portion is equivalent to the definition given in (1) and represents the average power consumption (constant energy flow per unit time supplied to the circuit (load) through a PCC).

$$Q = \boldsymbol{V}\boldsymbol{I}_r^b = \sqrt{\left(V_a^2 + V_b^2 + V_c^2\right)\left(I_{ra}^{b\,2} + I_{rb}^{b\,2} + I_{rc}^{b\,2}\right)} \tag{17}$$

is the ***reactive power.*** It is also easy to show that Q can be expressed by:

$$Q = \frac{\boldsymbol{V}}{\hat{\boldsymbol{V}}} W_r = \omega W_r \sqrt{\frac{1 + THD_v}{1 + THD_{\hat{v}}}} \tag{18}$$

where ω is the angular line frequency, THD_v is total harmonic distortion of the voltages and similarly $THD_{\hat{v}}$ is total harmonic distortion of the unbiased voltage integrals. Eq. (18) shows that, unlike reactive energy W_r, reactive power Q is not conservative. In fact, it depends on line frequency and (local) voltage distortion. This remark is important for modern microgrids, where voltage distortion and frequency variations can be non negligible. Reactive power is conservative only for sinusoidal conditions and constant line frequency. Only in sinusoidal condition (17) has the same value as the reactive power defined by the standard STD 1459 [3].

$$N = \boldsymbol{V}\boldsymbol{I}^u = \sqrt{\left(V_a^2 + V_b^2 + V_c^2\right)\left(I_a^{u\,2} + I_b^{u\,2} + I_c^{u\,2}\right)} \tag{19}$$

is the ***unbalanced power***, and is uniquely associated with unbalanced load behavior (different values of conductance and reactivity of phase). In single-phase circuits, this component disappears.

$$D = \boldsymbol{V}\boldsymbol{I}_v = \sqrt{\left(V_a^2 + V_b^2 + V_c^2\right)\left(I_{va}^2 + I_{vb}^2 + I_{vc}^2\right)} \tag{20}$$

is the ***void (distortion) power***, which is related with the non-linearity between voltage and current (existence of non-linear behavior).

Finally from (4) and (15) the ***power factor*** results:

$$\lambda = \frac{P}{\sqrt{P^2 + Q^2 + N^2 + D^2}} \tag{21}$$

From (21) it is observed that the power factor relates the active power with all the other power terms through the apparent power, and results unity only in the case of load (circuit) purely resistive and balanced. Otherwise, the presence of energy storage elements, unbalanced loads and nonlinearities of load will influence (reduce) the power factor. Complementary analyses of the portions of currents and the related power components can be found in [5,11].

6. Applying CPT for analyzing three-phase X-ray machine

The decomposition method of the current/power discussed in the previous section was implemented in PSCAD™/EMTDC™ software and applied to the computational model of X-ray machine. Figs. 7 and 8, and Tables VI and VII show the results obtained at the measuring points PCC and the load terminals.

Observing the Figs. 7 and 8, and Table VI, it is possible to note that for all operation regions, there is not an unbalanced component (current and power), this is due to the symmetrical construction of the X-ray machine, that means the machine has a balanced characteristic. However, due to its non-linear characteristic void currents/power are present. Moreover, due to the different operation conditions, the amplitudes of the current terms (balanced active and reactive current, and the void current), and values of the power terms (active, reactive and distortion) increase on the area in which the machine operates. Area C (execution of X-ray radiography) presents maximum values and amplitudes.

The first column of Table VII shows the power factor ($P/A = \lambda$), computed be using the values reported in Table VI. The quantities Q/A, N/A and D/A, indicate how much power apparently is associated with reactive, unbalanced and distortion powers, respectively. It is observed that the distortion power in the Areas A and B has a higher value compared to reactive power, unlike C area, where the reactive power is higher. However, it is observed from the results that the distortion power is the most representative in all areas of operation, and it has almost the same value if the device is analyzed at the load terminals (office). Depending of the country this portion of power might not be billed.

On the other hand, the distortion power (void current) has a direct relationship with the total harmonic distortion in Tables II–V. As the void current contains all harmonic frequencies that do not generate active power neither reactive energy, these currents could be the time domain representation of the total harmonic distortion. Therefore, the collective rms value of the void current could be used to calculate the distortion index, which would be equivalent to THD for non-sinusoidal conditions. Thus, the distortion index based on the CPT is given by:

$$\lambda_D = \frac{D}{A} = \frac{\boldsymbol{I}_v}{\boldsymbol{I}} = \frac{\boldsymbol{I}_v}{\sqrt{\boldsymbol{I}_a^{b\,2} + \boldsymbol{I}_r^{b\,2} + \boldsymbol{I}^{u\,2} + \boldsymbol{I}_v^2}} \tag{22}$$

Note that, λ_D is obtained by collective rms values, and not by phase as shown in Tables II–V, which is usually done in most cases.

Just in case of balanced load supplied by sinusoidal voltages, λ_D can be associated with traditional current THD, by the ratio:

$$\lambda_D = \frac{THD_I}{\sqrt{1 + THD_I^2}} \tag{23}$$

For levels of total harmonic current distortion, up to 30%, the distortion factor is practically equal to the THD, in other words, $\lambda_D \cong THD_I$.

Similarly the traditional current unbalance factors (K_I^- and K_I^0), could be represented by the unbalance factor, defined as

$$\lambda_N = \frac{N}{\sqrt{P^2 + Q^2 + N^2}} = \frac{\boldsymbol{I}^u}{\sqrt{\boldsymbol{I}_2^{b\,2} + \boldsymbol{I}_r^{b\,2} + \boldsymbol{I}^{u\,2}}} \tag{24}$$

Note that, the unbalanced factor defined by the CPT current decomposition results in zero only if the load is balanced regardless of the voltages being balanced or distorted. Furthermore, the unbalance factor is a generic factor that considers both negative sequence

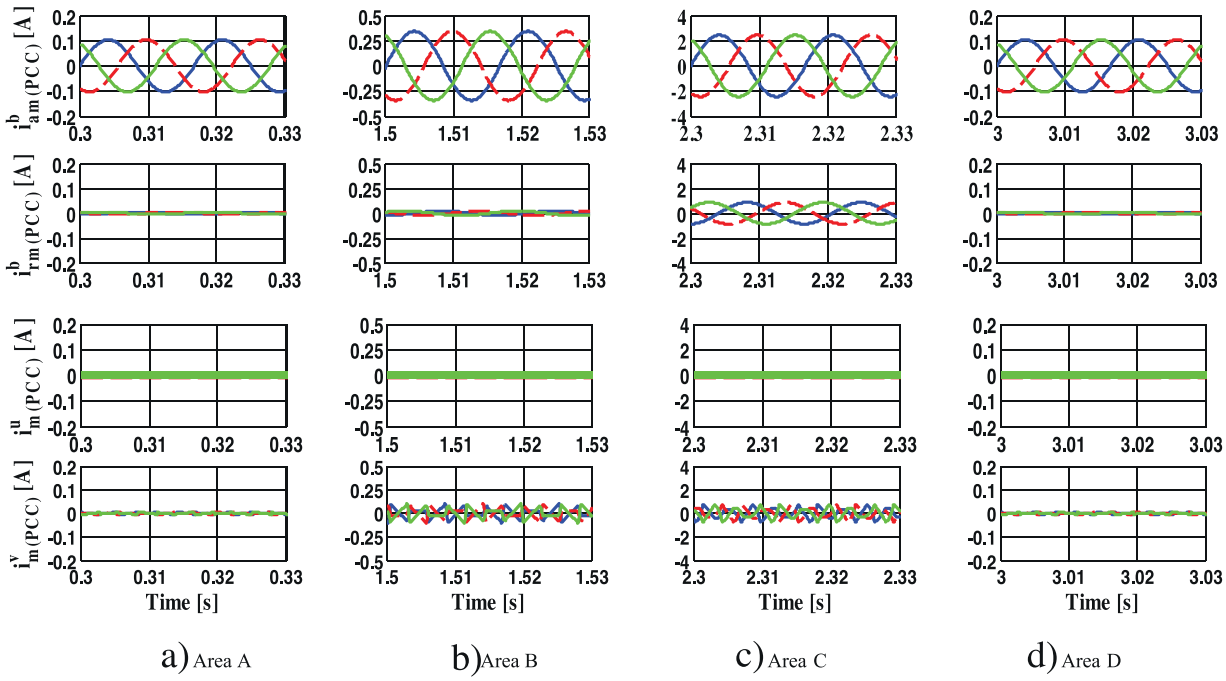

Fig. 7. Decomposition of the currents at PCC for each X-ray operation area.

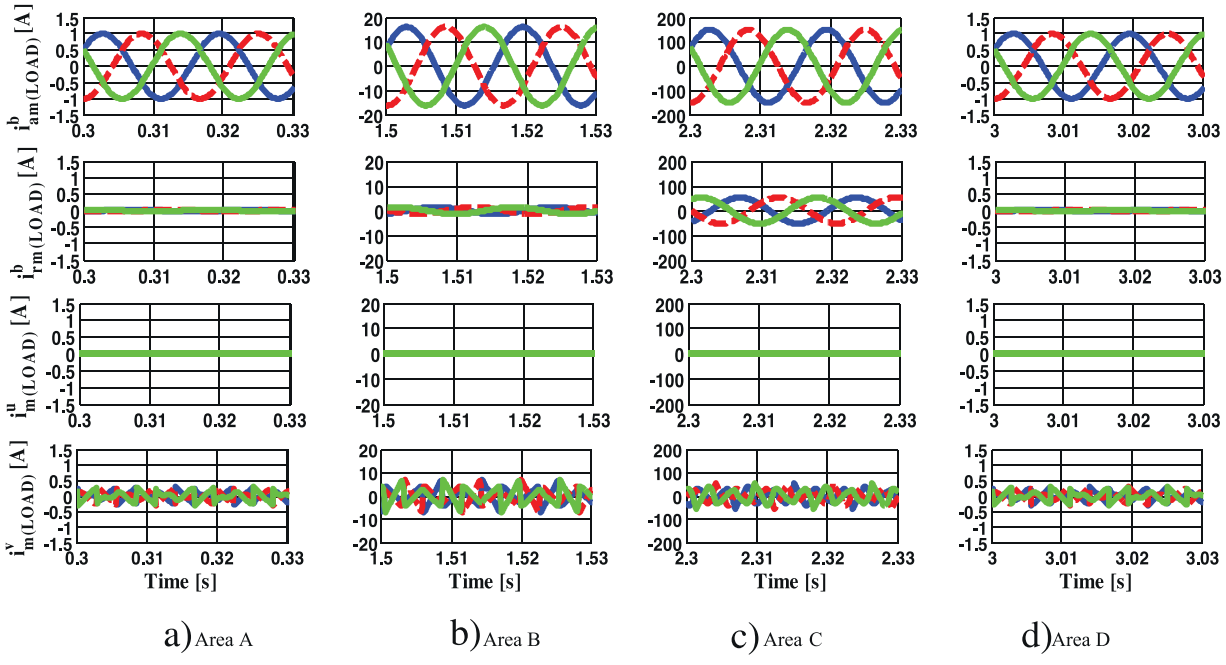

Fig. 8. Decomposition of the currents at load terminals for each X-ray operation area.

Table VI
Power terms and collective quantities.

	Area A		Area B		Area C		Area D	
	PCC	Load	PCC	Load	PCC	Load	PCC	Load
V (V)	13,802.70	220.00	13,802.40	219.92	13,799.10	218.49	13,802.40	220.00
I (A)	0.128	1.26	0.434	20.61	3.29	199.94	0.128	1.26
A (VA)	1772.67	276.56	5993.56	4531.82	45,363.84	43,685.60	1772.60	276.49
P (W)	1771.71	271.46	5.870.05	4368.40	41,919.30	40,286.40	1771.65	271.46
Q (VA)	4.20	3.96	376.09	368.57	14,675.10	14,148.30	3.98	3.75
N (VA)	0.00	0.00	0.05	0.04	0.02	0.01	0.00	0.00
D (VA)	58.24	52.71	1150.64	1148.36	9235.38	9233.83	57.95	52.40
λ	0.9994	0.9816	0.9794	0.9639	0.9241	0.9222	0.9995	0.9817

Table VII
Power terms indicators.

(pu)	Area A		Area B		Area C	
	PCC	Load	PCC	Load	PCC	Load
P/*A*	0.9994	0.9816	0.9794	0.9639	0.9241	0.9222
Q/*A*	0.0024	0.0143	0.0627	0.0813	0.3235	0.3239
N/*A*	0.0000	0.0000	0.0000	0.0000	0.0000	0.0000
D/*A*	0.0328	0.1906	0.1920	0.2534	0.2036	0.2114

components as the components of zero sequence, regardless of current's waveform (sinusoidal asymmetric and/or nonsinusoidal asymmetric) [22]. Of course, in the case of single-phase circuits this factor is irrelevant resulting in zero.

Only in case of unbalanced load, being supplied by symmetrical sinusoidal voltages (balanced), λ_N may be associated with traditional factors of unbalanced conditions, by the relation:

$$\lambda_N = \sqrt{\frac{K_I^{-2} + K_I^{02}}{1 + K_I^{-2} + K_I^{02}}} \tag{25}$$

It is observed that in the case of unbalanced three-phase circuits without a return conductor (three wire), Eq. (25) results:

$$\lambda_N = \frac{K_I^-}{\sqrt{1 + K_I^{-2}}} \tag{26}$$

Thus, λ_N considers only the negative sequence components.

The traditional displacement factor, $\cos\phi$, used in the analysis of sinusoidal signals, also could be generalized to analyze electrical circuits under non-sinusoidal conditions by the reactivity factor, defined in (27):

$$\lambda_Q = \frac{P}{\sqrt{P^2 + Q^2}} = \frac{\boldsymbol{I}_a^{b\,2}}{\sqrt{\boldsymbol{I}_a^{b\,2} + \boldsymbol{I}_r^{b2}}} \tag{27}$$

It is observed that, regardless of the signals waveforms of the voltages and currents, λ_Q indicates the phase displacement between the voltages and currents caused by energy-storage elements (inductors and capacitors) or even by non-linear loads. Moreover, the reactivity factor is an equivalent factor, which represents the phase shift of voltage and current collectively.

The reactivity factor has a direct relationship with the displacement factor only when the signals of voltage and the current are perfectly sinusoidal:

$$\lambda_Q = \cos\,\phi \tag{28}$$

It is important to note that, depending on the application and the necessary analysis, all the conformity factors (performance indexes) of the load, based on CPT, i.e., λ_D, λ_N and λ_Q, can also be calculated for each phase by phase values.

Finally, from Eqs. (22), (24) and (27) can easily be shown that:

$$\lambda = \lambda_Q \sqrt{\left(1 - \lambda_N^2\right)\left(1 - \lambda_D^2\right)} = \frac{\boldsymbol{I}_a^b}{\boldsymbol{I}} \tag{29}$$

It is observed that, (29) results in unitary only if the load is purely resistive and balanced, regardless of the supply voltages. In addition, a pure balanced resistive load can have a unit power factor, even in the presence of nonsinusoidal and/or asymmetrical voltages. Thus, the presence of any other type of disturbances (phase shift, unbalances and/or harmonics) affects the power factor.

Finally, to the condition of sinusoidal voltage the power factor, results:

$$\lambda = \cos\,\phi \sqrt{\left(\frac{1}{1 + THD_I^2}\right)\left(\frac{1}{1 + K_I^{-2} + K_I^{02}}\right)} \tag{30}$$

Table VIII
Performance indicators.

	Area A		Area B		Area C	
	PCC	Load	PCC	Load	PCC	Load
λ_Q	1.000	1.000	0.998	0.996	0.944	0.943
λ_N (%)	0.000	0.000	0.000	0.000	0.000	0.000
λ_D (%)	3.20	19.10	19.20	25.30	20.30	21.10

In case of three-phase circuits three-wire (without return conductor), the previous Eq. (30) can still be reduced to:

$$\lambda = \cos\phi \sqrt{\left(\frac{1}{1 + THD_I^2}\right)\left(\frac{1}{1 + K_I^{-2}}\right)} \tag{31}$$

All the indexes, (22), (24) and (27) obtained by the power and currents decomposition of the CPT to the X-ray machine are listed in Table VIII. Under ideal operation, the distortion factor (λ_D) is zero, similarly to the total harmonic distortion (THD), since it expresses the absence of nonlinearities, λ_N is also zero, similarly to the unbalanced factors (negative and zero sequence), since it expresses the effects of unbalanced loads and whereas the reactivity factor (λ_Q) and power factor (λ) result unitary, similarly to the traditional displacement factor, since it express the circuit efficiency. Note that, the distortion factor (λ_D) information in Table VIII is related to the entire three-phase circuit (equivalent circuit), not to single phase variables, that is the case of the Tables II–V.

7. Impact of X-ray on electric power distribution systems

As noted in the previous section, the X-ray machine when triggered, depending upon operating mode and the electric power supply condition, can cause voltages sags, current distortions or even fast voltage fluctuations, and it may cause "flicker" [7,8]. Moreover, it turns out that during the radiography's execution the levels of current are high, requiring a large amount of power absorbed from the grid in a non-continuous operation. The Brazilian standard technical guidance proposed in [8] defines three basic types of operating modes for X-ray machines:

- *Consecutive exhibitions regime, slow pace*: it is the case of radiography in general, where several plates are taken with an interval between one position and another around 50 s. This time depends on the type of the device and its minimum value must be provided by the user;
- *Consecutive exhibitions regime, fast pace*: it is a technique called fast serioscopy, using a heat exchanger film or a quick photographic camera, it can obtain a series from 5 to 30 exposures in a time of 10–30 s;
- *Cine regime, pulse*: it consists of using the X-ray generator synchronized to a video camera, doing a little exposure for each image of the film. Depending on the device, one can have records of 10 s at a speed of 60 images per second.

The operation mode of the machine must be specified on the forms required by the utility supply for the connection of this type of load to the electrical system. However, it should be highlighted that in the case of operating on the consecutive exhibitions regime, the device will consume active power, reactive power and distortion power in a non-continuous mode, several times during the day.

Therefore, to provide active power, *P* at a given load, any deviation of power from a balanced purely resistive load (equal resistance to all three phases) increases transmission losses. To take account the increase in transmission losses, we can define the line

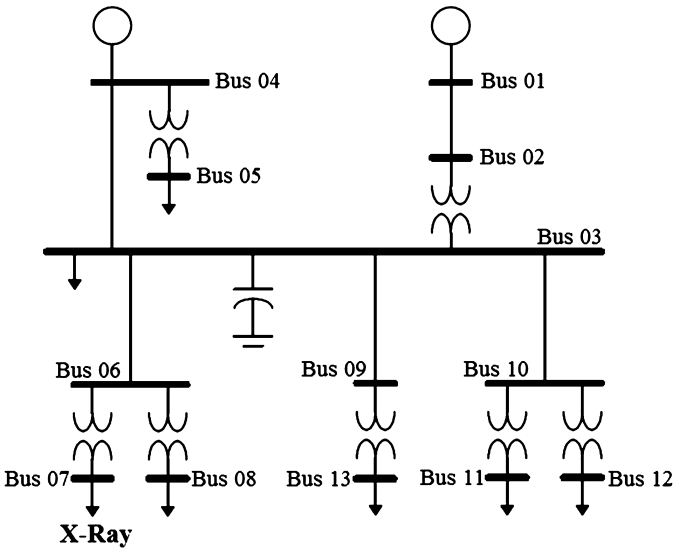

Fig. 9. Single line diagram of IEEE 13 bus distribution system [20].

utilization factor, K_{line} (losses) as the ratio between the total losses (P_{total}) and minimum transmission losses (P_{min}):

$$K_{line} = \frac{P_{total}}{P_{\min}} \tag{32}$$

Note that, the above equation is generic, applicable to any operating condition. Furthermore, $K_{line} = 1$ only when the circuit (load) is balanced purely resistive (voltages and currents are in phase).

For a generic three-phase circuit (linear or not), the definition of power factor given in (29) can be used to calculate the increase in transmission loss, since it is proportional to the square of the collective rms values of currents and voltages. Thus, considering (16), the minimum transmission losses results:

$$P_{min} = R_{line}\boldsymbol{I}_{min}^2 = R_{line}\left(\frac{P}{\boldsymbol{V}}\right)^2 = R_{line}\boldsymbol{I}_a^{b\,2} \tag{33}$$

and considering (13), the total loss is given by:

$$P_{total} = R_{line}\boldsymbol{I}^2 = R_{line}\left(\boldsymbol{I}_a^{b\,2} + \boldsymbol{I}_r^{b2} + \boldsymbol{I}^{u\,2} + \boldsymbol{I}_v^2\right) \tag{34}$$

Substituting (34) and (33) into (32) we have:

$$K_{line} = \frac{\boldsymbol{I}_a^{b\,2} + \boldsymbol{I}_r^{b2} + \boldsymbol{I}^{u\,2} + \boldsymbol{I}_v^2}{\boldsymbol{I}_a^{b\,2}} = \frac{1}{\lambda^2} \tag{35}$$

or, considering the load performance index defined in (22), (24) and (27) we have:

$$K_{line} = \frac{1}{\lambda_Q^2\left(1-\lambda_N^2\right)\left(1-\lambda_D^2\right)} \tag{36}$$

The above equation clearly shows how the reactivity, unbalanced and distortion factors increase the line utilization factor, enlarging line losses. For most applications, Eqs. (35) and (36) give acceptable results, but one should be aware of its limitations. The line resistance was assumed to be independent of frequency. However, for sharp harmonics or high frequency distortions that assumption may not be sufficiently precise. Similarly, to the shunt components losses it was assumed constant conductance, when neither hysteresis nor parasitic losses are proportional to the square of the rms voltage (or flux density). Thus, the effects of field penetration or minor loops were not considered in Eqs. (35) and (36).

Table IX shows the values of the line utilization factor for different areas of operation of the X-ray device.

It is interesting to observe that, the effect of the X-ray machine in the line losses varies according to the operation area, getting to be 18% higher for the region where it is performed the radiography (Area C). This clearly shows that depending on the exhibitions regime: slow, fast or pulse exposure, regardless of point of connection, the X-ray machine will increase the losses instantaneously, intermittently throughout the day (month). Thus, stands out the necessity of specifying the operating regimes of the X-ray machine, enabling the utilities to have a control of the impacts of this device on the grid. Moreover, due to the operating regime of exhibitions, the device will consume reactive and distortion power several times during the day.

Table IX
Line utilization factor by X-ray machine.

	Area A		Area B		Area C	
	PCC	Load	PCC	Load	PCC	Load
K_{line}	1.001	1.038	1.042	1.077	1.170	1.177

7.1. Case study for IEEE 13 bus system

In order to analyze the voltage quality the IEEE industrial test system was considered. This test system was proposed by the IEEE Task Force on Harmonic modeling and simulation in [20]. This system has been specially modified in order to take into account the X-ray apparatus and four conditions is taken: Areas A, B, C and D according to the different areas of X-ray operation (Fig. 9).

Fig. 10 shows the effect of X-ray machine on voltage THD. As can be seen, for the case studied the voltage distortion levels are low, below 5%. However, different results are obtained depending on the choice of bus and the area of X-ray operation. Note that, during the radiography (Area C) it is observed the highest values of distortions at 7 bus, as well as the others bus. The total harmonic distortion in all bus can be considered low (below 5%).

Fig. 11 summarizes the voltage profile of the buses. It can be seen that all the bus voltages are within the acceptable level (±5%), some standards consider (±10%). The lowest voltage compared to the other buses can be noticed in bus number 7. Note that, the rms voltage drops by almost 5% with respect to the reference value (1 pu) during Areas A and D. The X-ray has little impact on rms voltages as can be seen in bus 7. It is clearly that depending on the exhibitions regime the voltage profile will be changed.

Fig. 12 shows the effect of X-ray machine on current THD. It can be seen clearly that bus 7 is the most critical bus compared to the

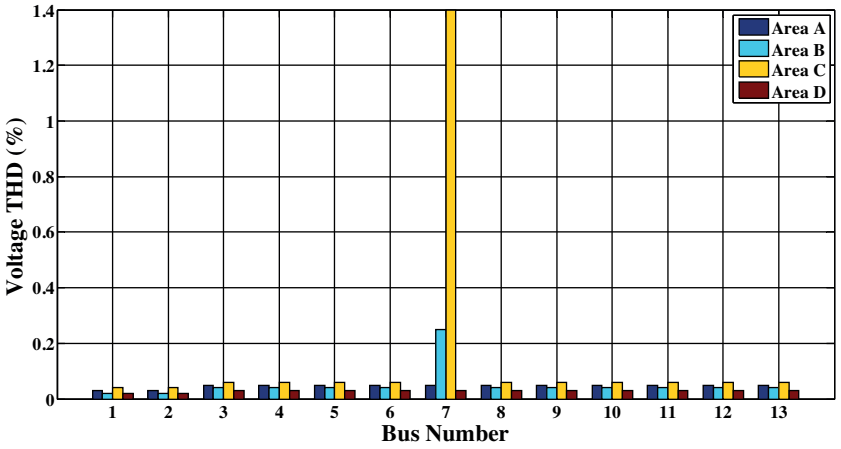

Fig. 10. Effect of X-ray on voltage THD.

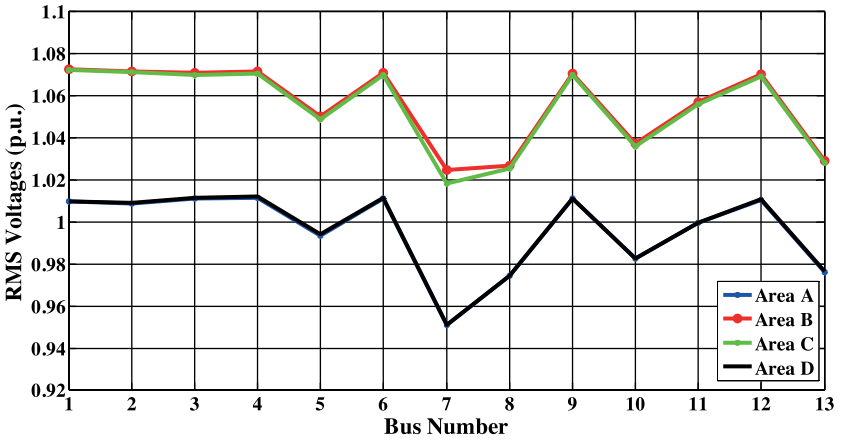

Fig. 11. Voltage profiles of all buses of the IEEE 13 bus system.

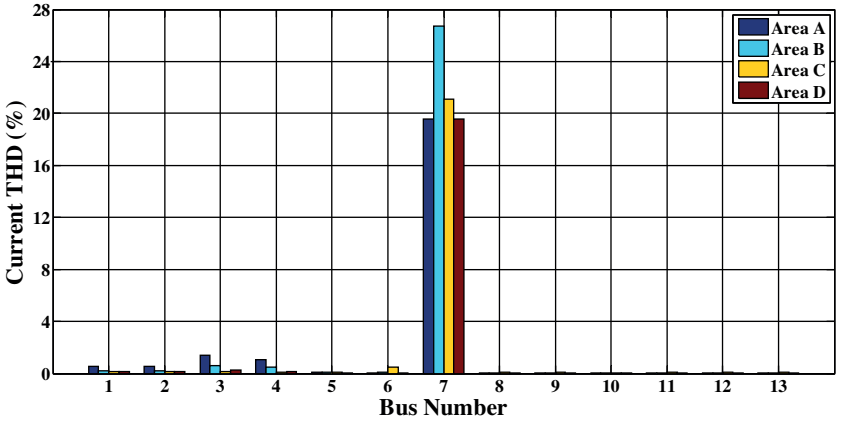

Fig. 12. Effect of X-ray on current THD.

other buses. It is well evidenced that bus 7 which have the X-ray machine is the origin of distortion.

Note that, from Fig. 12 the current THD values oscillated between 18% and 27% at bus 7 in the same way as presented in electrical network of Fig. 3. These harmonic currents will cause additional line losses and stray losses in transformer and possible equipment loss-of-life, as well as, overcurrent or overvoltage resulting from resonances due to the capacitor connected at bus 3.

8. Conclusions

It is verified that the X-ray equipment works as a disturbing load for the power supply. By applying the conservative power theory and using field measurements and simulation results it was possible to identify the load characteristics and the potential impacts on power quality and line loss due to this type of disturbing load. The developed model implemented in PSCAD™/EMTDC™ software can be used to power quality studies, load connection evaluation,

power factor correction, for selecting the point of common coupling, for resonance analysis, for evaluating the time-varying characteristics of harmonics and cost of solutions (cost/benefit analysis).

Through the currents analysis, it is found that the disturbing load can be tariffed and accountable for the amount of harmonics generated in the executions of radiographs. Each operation requires a large amount of power, which causes voltage sags in the PCC, while damaging other consumers connected at this point, besides the issue of harmonics.

In this way, a study including diagnosis and conditions for connecting disturbing loads to the electrical system [6] was performed, as well as the means to tariff and punish the disturbing load which deteriorates the electrical power quality and power system.

Finally, the performance factors based on the CPT current/power describe particular load phenomena or characteristics. Thus these factors can be used as an alternative for evaluating the power quality of particular noisy loads or installations, instead of the traditional total harmonic distortion, negative and zero sequence indexes. Such conventional quantities are related to the currents waveforms and not specifically to the load characteristics.

Acknowledgements

The authors wish to express their gratitude to FAPESP (São Paulo Research Foundation, Process 2013/08545-6) for supporting this research.

References

[1] I.M. Nejdawi, A.E. Emanuel, D.J. Pileggi, M.J. Corridori, R.D. Archambeault, Harmonics trend in NE USA: a preliminary survey, IEEE Trans. Power Deliv. 14 (October (4)) (1999) 1488–1494.
[2] Union of the Electricity Industry – EURELECTRIC, Power Quality in European Electricity Supply Networks, 2nd ed., 2003.
[3] IEEE Standard Definitions for the Measurement of Electric Power Quantities Under Sinusoidal, Nonsinusoidal, Balanced, or Unbalanced Conditions, IEEE Std 1459-2010 (Revision of IEEE Std 1459-2000), 2010, pp. 1–50.
[4] C. Muscas, Power quality monitoring in modern electric distribution systems, IEEE Instrum. Meas. Mag. 13 (October) (2010) 19–27.
[5] P. Tenti, H.K.M. Paredes, P. Mattavelli, Conservative power theory, a framework to approach control and accountability issues in smart microgrids, IEEE Trans. Power Electron. 26 (March (3)) (2011) 664–673.
[6] IEEE Draft Guide for Applying Harmonic Limits on Power Systems, IEEE P519.1/D12, July 2012, 2015, pp. 1–124.
[7] M.C.G. Ramos, C.M.V. Tahan, An assessment of the electric power quality and electrical installation impacts on medical electrical equipment operations at health care facilities, Am. J. Appl. Sci. (2009) 638–645.
[8] CPFL Energy: 'Technical Orientation – Criterion to Meet the X-ray Apparatus', Document n. 239, Version 1.1, September, 2006 (in Portuguese).
[9] EN 50160: "Voltage Characteristics of Electricity Supplied by Public Distribution Systems", European Standard, 1996.
[10] IEC 61000-3-6: "Electromagnetic Compatibility (EMC) – Part 3: Limits – Section 6: Assessment of Emission Limits for Distorting Loads in mv and hv Power Systems", Basic EMC Publication, 1996.
[11] P. Tenti, P. Mattavelli, H.K.M. Paredes, Conservative Power Theory Sequence Components and Accountability in Smart Grids, International School on Nonsinusoidal Currents and Compensation (ISNCC), 2010, pp. 37–45.
[12] V. Staudt, Fryze-Buchholz-Depenbrock: a time-domain power theory, Przegląd Elektrotechniczny (Electr. Rev.) 6 (2008) 1–11.
[13] F.P. Marafão, E.V. Liberado, H.K.M. Paredes, L.C.P. da Silva, Three-phase four-wire circuits interpretation by means of different power theories, International School on Nonsinusoidal Currents and Compensation (ISNCC) (2010 June) 168–173.
[14] H.K.M. Paredes, F.P. Marafão, L.C.P. da Silva, A Comparative Analysis of FBD, PQ and CPT Current Decompositions Part I: Three-phase, Three-wire Systems, IEEE PowerTech, Bucharest, 2009, pp. 1–6.
[15] L.S. Czarnecki, Currents' physical components (CPC) concept: a fundamental of power theory, Przegląd Elektrotechniczny (Electr. Rev.) (6) (2008) 28–37.
[16] J.L. Willems, Reflections on power theories for poly-phase nonsinusoidal voltages and currents, Przegląd Elektrotechniczny (Electr. Rev.) (6) (2010) 11–21.
[17] A.C. Moreira, L.C.P. da Silva, H.K.M. Paredes, Electrical modelling and power quality analysis of three-phase X-ray apparatus, in: 22nd International Symposium on Power Electronics, Electrical Drives, Automation and Motion (SPEEDAM), Ischia, Italy, June 2014, pp. 1098–1103.
[18] Fundamentals of X-ray Physics, U.S. Army Medical Department Center and School Fort Sam Houston, Texas.
[19] H.K.M. Paredes, F.P. Marafão, P. Mattavelli, P. Tenti, Application of conservative power theory to load and line characterization and revenue metering, in: IEEE International Workshop on Applied Measurements for Power Systems (AMPS), September 2012, pp. 1–6.
[20] Task force on harmonics modelling and simulations: "test systems for harmonics modeling and simulation", IEEE Trans. Power Deliv. 14 (April 2) (1999) 579–587.
[21] P. Tenti, E. Tedeschi, P. Mattavelli, Compensation techniques based on reactive power conservation, Electr. Power Qual. Util. XIII (1) (2007) 17–24.
[22] F.P. Marafão, W.A. Souza, E.V. Liberado, L.C.P. da Silva, H.K.M. Paredes, Load analyser using conservative power theory, Przeglad Elektrotechniczny (2013) 1–6.